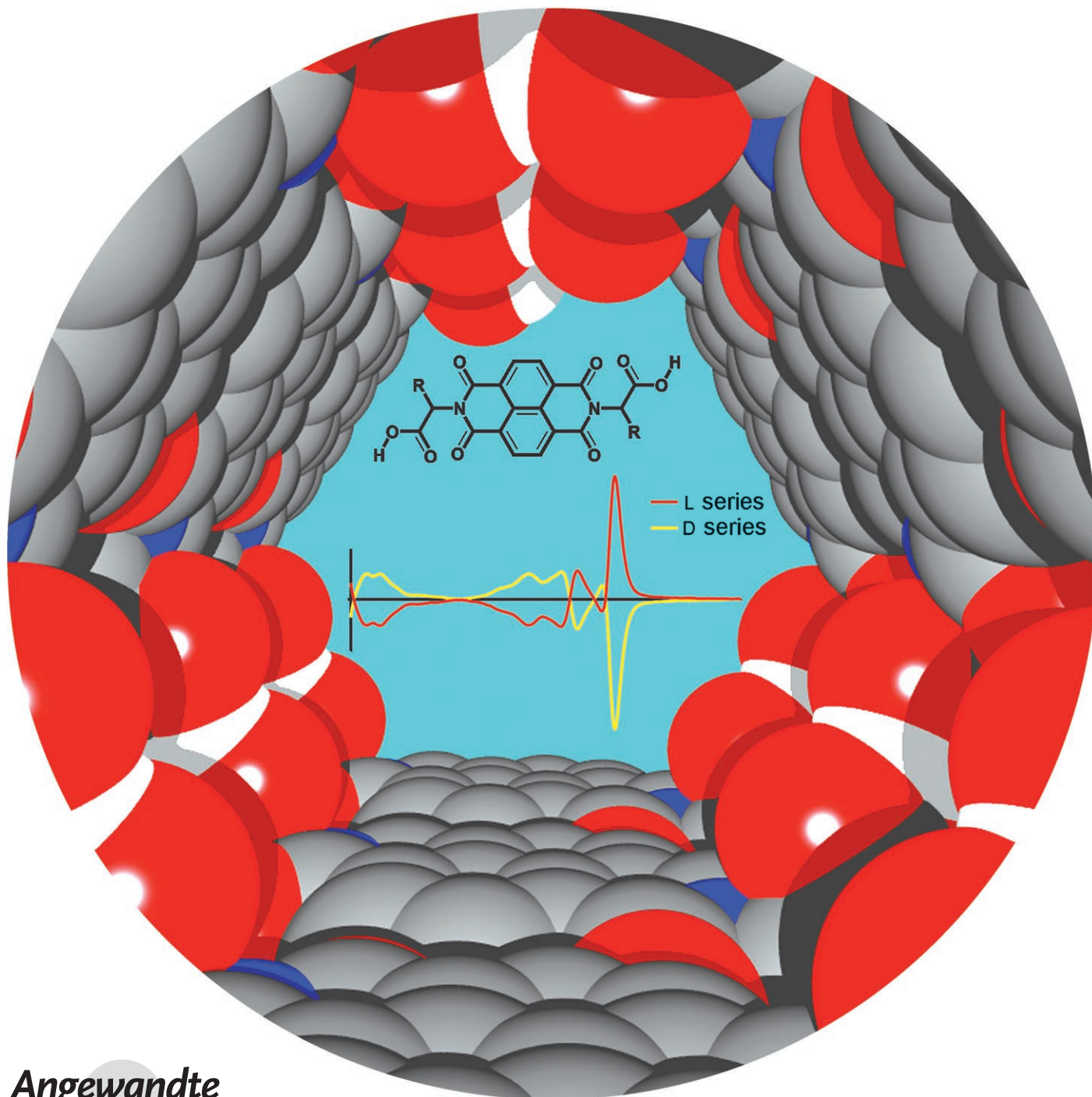


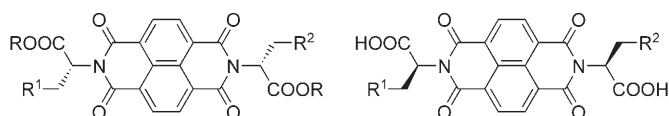
# Hydrogen-Bonded Helical Organic Nanotubes\*\*

G. Dan Pantoş, Paolo Pengo, and Jeremy K. M. Sanders\*



We report herein the discovery of a new class of noncovalent polymers<sup>[1]</sup> that form helical nanotubes in nonpolar solution and in the solid state. These structures are simple to prepare, they possess a uniform core with the potential to bind a variety of guests, and they display externally a range of side chains that currently are derived from amino acid residues. The structural requirements defined by the results detailed below are simply a *N,N'*-dimethylnaphthalenediimide with a pendant carboxylic acid.

The synthesis of compounds **1–7** was carried out by using microwave dielectric heating of reaction mixtures containing 1,4,5,8-naphthalenetetracarboxylic anhydride and the corresponding amino acid under the conditions previously reported by us (see Scheme 1 and the Supporting Information).<sup>[2]</sup>



L-1:  $R^1 = R^2 = \text{STrt}$ ,  $R = \text{H}$

L-2:  $R^1 = R^2 = \text{OBzl}$ ,  $R = \text{H}$

L-3:  $R^1 = R^2 = (\text{CH}_2)_3\text{NHBoc}$ ,  $R = \text{H}$

4:  $R^1 = R^2 = \text{STrt}$ ,  $R = \text{Me}$

5:  $R^1 = \text{STrt}$ ,  $R^2 = \text{OBzl}$ ,  $R = \text{H}$

6:  $R^1 = \text{CH}_2\text{CO}_2\text{tBu}$ ,  $R^2 = \text{CH}_2\text{CONHtEt}$ ,  $R = \text{H}$

7:  $R^1 = (\text{CH}_2)_3\text{NHAc}$ ,  $R^2 = (\text{CH}_2)_3\text{NHBoc}$ ,  $R = \text{H}$

D-1:  $R^1 = R^2 = \text{STrt}$

D-2:  $R^1 = R^2 = \text{OBzl}$

D-3:  $R^1 = R^2 = (\text{CH}_2)_3\text{NHBoc}$

**Scheme 1.** Amino acid NDI derivatives. Boc = *tert*-butoxycarbonyl, Bzl = benzyl, Trt = trityl.

Structural proof for compound **L-1** came from X-ray diffraction analysis of the crystals grown by slow evaporation from a dichloromethane solution of **L-1** (Figure 1).<sup>[3]</sup> This compound crystallizes in the  $P3_1$  space group in which the amino acid side chains adopt a *syn* geometry with respect to the naphthalenediimide (NDI) plane. This geometry allows three *S*-trityl groups of three different molecules to interdigitate and the carboxylic groups of **L-1** to dimerize through two strong intermolecular hydrogen bonds ( $\text{O1}'\text{H}\cdots\text{O2}''$ , 2.61 Å, 161° and  $\text{O1}''\text{H}\cdots\text{O2}'$ , 2.63 Å, 161°). Closer inspection of the crystal structure reveals that **L-1** assembles in a hydrogen-bonded nanotubular supramolecular structure, in which NDI cores *i* and *i* + 3 are coplanar with each other, forming the walls of the nanotube (Figure 2, Scheme 2). This structure is reinforced by two weak  $\text{C}\cdots\text{H}\cdots\text{O}$  hydrogen-bond interactions ( $\text{C10H}\cdots\text{O2}$ , 3.16 Å, 142° and  $\text{C4H}\cdots\text{O4}$ , 3.15 Å, 143°) per

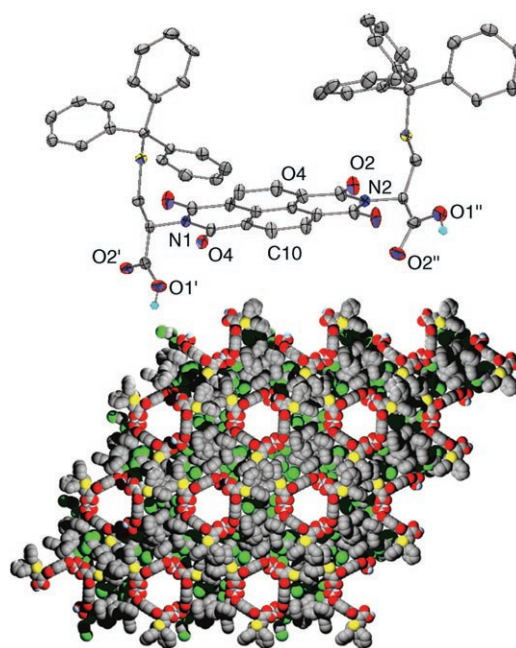


**Figure 1.** Side and top views of the crystal packing of **L-1**. Thermal ellipsoids are scaled at the 50% probability level. Most of the hydrogen atoms and water molecules have been removed for clarity.

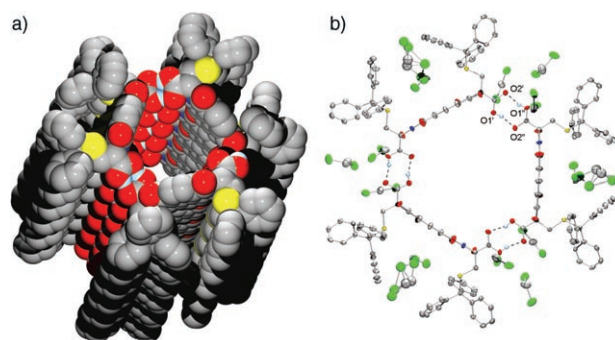


**Figure 2.** Side and top views of the hydrogen-bonded nanotubular structure formed by **L-1**. Thermal ellipsoids are scaled at the 50% probability level. Most of the hydrogen atoms, water molecules (a, b), and  $\text{CH}_2\text{Cl}_2$  molecules (a) have been removed for clarity.

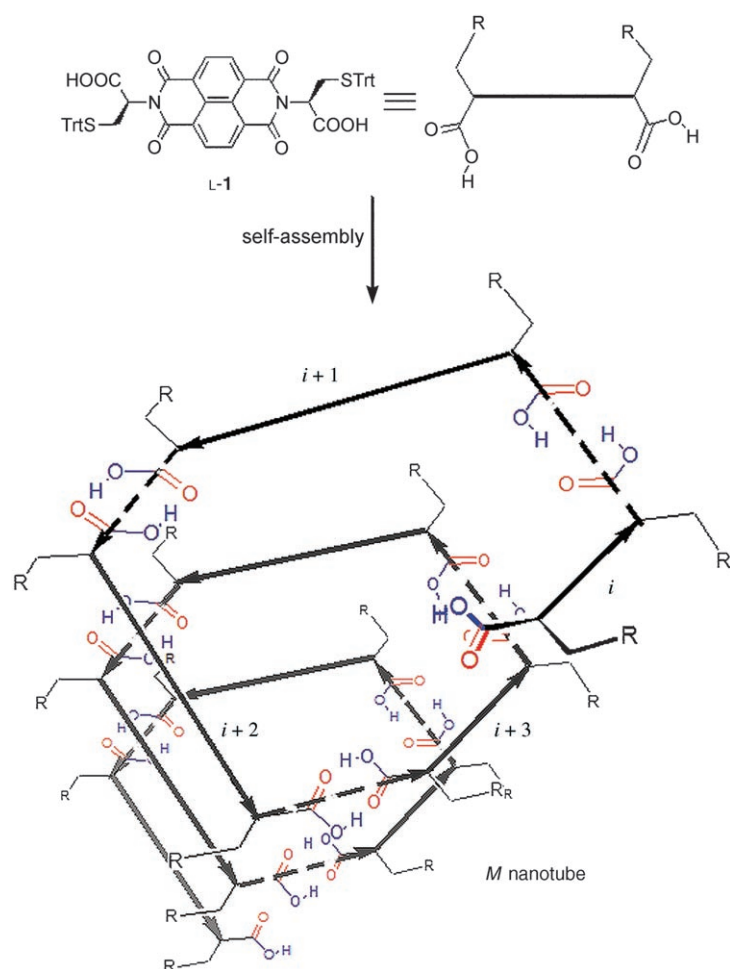
unit, again formed between NDIs *i* and *i* + 3 that form the walls of the nanotube. In this arrangement, the angle between the central  $\text{N1}\text{--}\text{N2}$  axis of the NDI core and the central axis of the nanotube is 60°, whereas the distance between two sequential aromatic cores is on average 4.8 Å. The inner diameter of the nanotube is on average 12.4 Å and it contains diffused water molecules.

An important feature of this assembly is the uniform supramolecular stereochemistry of the nanotubes. As depicted in Scheme 2, compound **L-1** has the *R,R* absolute stereochemistry at the two stereocenters provided by the amino acid side chains, and it assembles in the solid state uniformly into *M*-helical nanotubes throughout the crystalline lattice. Chiroptical solution studies of **L-1** confirm that the helical structure observed in the solid state was maintained in aprotic solvents such as chloroform. Comparing the CD spectra (Figure 3), it can be seen that although **L-1** (blue

[\*] Dr. G. D. Pantoş, Dr. P. Pengo, Prof. J. K. M. Sanders  
University Chemical Laboratory  
University of Cambridge  
Lensfield Road, Cambridge CB21EW (UK)  
Fax: (+44) 1223-336-017  
E-mail: jkms@cam.ac.uk

[\*\*] We thank Dr. Sijbren Otto, Mr. Jean-Luc Wietor, and Mr. Andrew J. Baldwin for helpful discussions, Dr. J. E. Davis for crystal structures, and EPSRC for financial support.

Supporting information for this article is available on the WWW under <http://www.angewandte.org> or from the author.



**Scheme 2.** Representation of self-assembled nanotubes composed of NDI units. The arrows indicate the direction of the nanotube assembly.

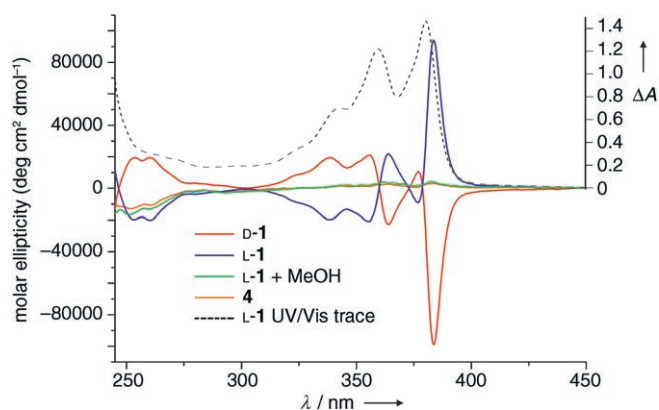


**Figure 3.** CD spectra of L-1, D-1, and **4** in CHCl<sub>3</sub> solution and of L-1 in CHCl<sub>3</sub> in the presence of 500 equivalents of MeOH (green trace). Black trace: UV/Vis spectrum of L-1 in CHCl<sub>3</sub> ( $4.6 \times 10^{-5}$  M).

trace) and **4** (orange trace) have similar behavior between 250–300 nm, L-1 displays a strong Cotton effect above 300 nm that corresponds to the UV/Vis absorption of the NDI core. This can be ascribed to the formation of a chiral supramolecular structure like that observed in the solid state, in which the NDI units are arranged in such a way that gives rise to an induced Cotton effect (ICD) with a maximum at 383 nm.

Furthermore the *R,R* (**L-1**) and the *S,S* (**D-1**, red trace) enantiomers have opposite CD behavior, indicating the formation of a supramolecular structure with similar geometry but opposite chirality. The molar ellipticities of **L-1** and **D-1** in anhydrous CHCl<sub>3</sub> were around  $-9.5 \times 10^4$  and  $+9.5 \times 10^4$  deg cm<sup>2</sup> dmol<sup>-1</sup> at 383 nm, respectively.

The chiroptical properties of compounds **L-2**, **D-2**, **L-3**, and **D-3** were also examined by CD measurements (see the Supporting Information). The molar ellipticities in anhydrous CHCl<sub>3</sub> at the maximum ICD are  $3 \times 10^4$  and  $4 \times 10^4$  deg cm<sup>2</sup> dmol<sup>-1</sup> for **L-2** and **L-3**, respectively, and  $-3 \times 10^4$  and  $-4 \times 10^4$  deg cm<sup>2</sup> dmol<sup>-1</sup> for **D-2** and **D-3**, respectively.

Proof for the hydrogen-bonded supramolecular nature of the helical nanotubes came from the CD spectrum of a CHCl<sub>3</sub> solution **L-1** in the presence of 500 equivalents of methanol (green trace): this is identical with the spectrum of **4**, a reference compound that cannot form hydrogen-bonded structures (see the Supporting Information). This indicates the destruction of the supramolecular structure upon addition of a protic solvent capable of hydrogen-bond interactions. Similar results were obtained for compounds **D-1**, **L-2**, **D-2**, **L-3**, and **D-3**. This supports the idea that regardless of the nature of the amino acid side chain, these compounds form supramolecular nanotubes through a network of hydrogen bonds.

The formation of the helical nanotubular structures is independent of the symmetry of the substitution pattern on the NDI core as demonstrated by the CD spectra of the three unsymmetrical derivatives, **5–7** (Figure 4). The molar ellipticities for the unsymmetrical compounds are  $8 \times 10^4$  deg cm<sup>2</sup> dmol<sup>-1</sup> for **5**,  $2 \times 10^4$  deg cm<sup>2</sup> dmol<sup>-1</sup> for **6** in the presence of 300 equivalents acetone, and  $4.5 \times 10^3$  deg cm<sup>2</sup> dmol<sup>-1</sup> for **7** in the presence of 1000 equivalents acetone, in dry CDCl<sub>3</sub>; the acetone was added for solubility reasons.

There is consistency in the supramolecular chiral induction: **L-1**, **L-2**, **L-3**, and **5–7** all give CD spectra of the same sense, showing that an L-amino acid derivative of NDI will form, in aprotic solvents, an *M*-helical nanotube, whereas the *D* derivative will form the *P* nanotube. The persistence of ICD at concentrations as low as  $7.4 \times 10^{-6}$  M confirms that carboxylic acid hydrogen bonding is augmented by additional interactions, presumably those observed in the solid state.

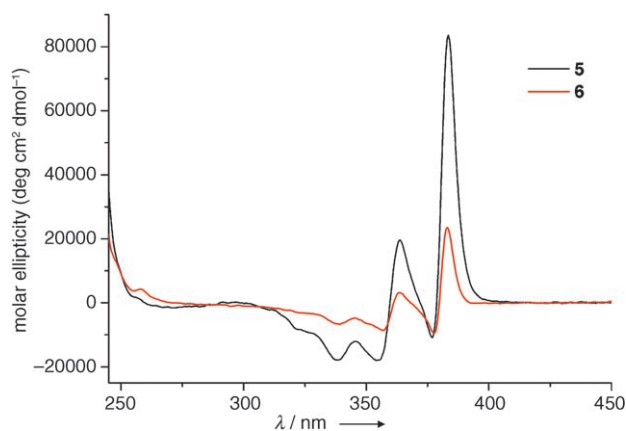


**Figure 4.** CD spectra of **5** and **6** in the presence of 300 equivalents of acetone in CHCl<sub>3</sub> solution.



The unsymmetrical compounds **5–7** were probed by 2D NMR spectroscopy. Figure 5 shows a section of the ROESY spectra of  $[D_8]$ toluene (a) and  $[D_4]$ methanol (b) solutions of **5**. In  $[D_8]$ toluene, the  $CH_3$  signal of the cysteine *S*-*tert*-butyl group (1.2 ppm) is connected with the phenyl CH protons (7.2–7.1 ppm) of the O-benzyl group of the serine

helical nanotubes. These compounds represent a major advance in this field, not only through their synthesis and formation independent of the amino acid sidechains, but also by being versatile in their room for structural variation and side chain decoration on the surface in a manner reminiscent of phage display. Currently we are investigating possible applications for these new materials.

Received: August 16, 2006

Published online: November 7, 2006

**Keywords:** helical structures · nanotubes · polymers · self-assembly · supramolecular chemistry

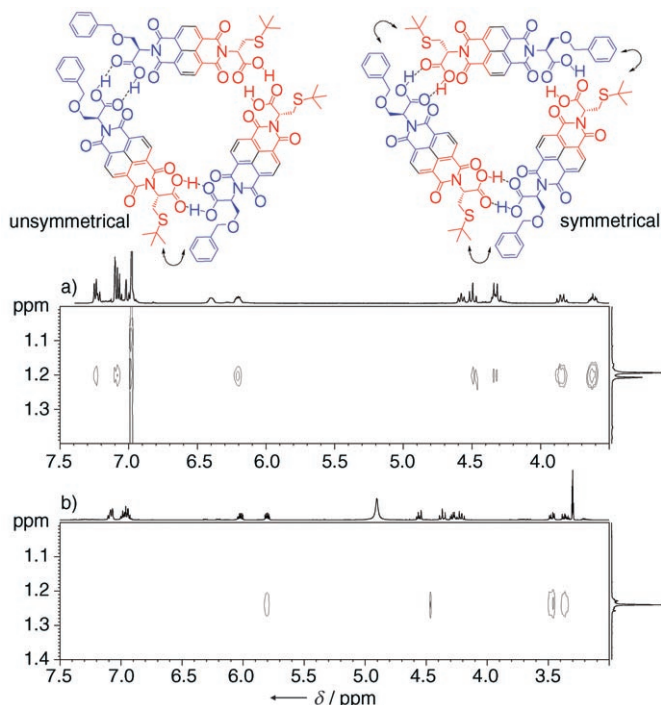


**Figure 5.** Section of the ROESY spectra of  $[D_8]$ toluene (a) and  $[D_4]$ methanol (b) solutions of **5**. The top graphic depicts the top view of the two possible **5** nanotube arrangements.

residue; this indicates spatial proximity of the two protons, which is possible only if in the supramolecular structure a hetero cysteine–serine carboxylic dimer is formed (Figure 5). Of the two possible arrangements in which such interactions appear, the unsymmetrical formation is most likely to be present in solution as the cysteine *S*-*tert*-butyl  $CH_3$  protons are split into two singlets in a 2:1 ratio.<sup>[4]</sup> In  $[D_4]$ methanol, the  $CH_3$ –phenyl CH connectivity was not present and the cysteine *S*-*tert*-butyl  $CH_3$  signal appeared as a singlet, supporting an isotropic environment for these protons. These two observations provide a strong evidence for the presence of a monomeric species in protic solvent. Similar results were obtained from the ROESY spectra of **6** and **7** in  $[D_6]$ acetone and  $[D_4]$ methanol, respectively (see the Supporting Information).

We have demonstrated the formation of amino acid derived NDI hydrogen-bonded supramolecular organic nanotubes both in solution and in solid state. The chirality of the nanotubes is determined by the constituent amino acid, but is independent of the nature of the side chains. The field of nanotube research that has so far embraced single-walled carbon nanotubes,<sup>[5]</sup> organic nanotubes based on cyclic peptide oligomers,<sup>[6]</sup> nucleobases,<sup>[7]</sup> ureas,<sup>[8]</sup> carbohydrates,<sup>[9]</sup> calix[4]hydroquinones,<sup>[10]</sup> calixarenes,<sup>[11]</sup> and  $\pi$ -stacked assemblies<sup>[12]</sup> is expanded by these new easy-to-synthesize

- [1] *Supramolecular Polymers* (Ed.: A. Ciferri), Taylor & Francis, Boca Raton, **2005**; J.-M. Lehn, *Prog. Polym. Sci.* **2005**, *30*, 814–831; F. J. M. Hoebe, P. Jonkheijm, E. W. Meijer, A. P. H. J. Schenning, *Chem. Rev.* **2005**, *105*, 1491–1546.
- [2] P. Pengo, G. D. Pantoş, S. Otto, J. K. M. Sanders, *J. Org. Chem.* **2006**, *71*, 7063–7066.
- [3] Crystallographic data for **L-1**:  $C_{63}H_{57}Cl_{10}N_2O_{10.5}S_2$ ,  $M_r = 1428.73$ ,  $0.35 \times 0.23 \times 0.16 \text{ mm}^3$ , trigonal,  $a = 26.6288(5)$ ,  $b = 26.6288(5)$ ,  $c = 9.0055(1) \text{ Å}$ ,  $V = 5530.21(16) \text{ Å}^3$ , space group  $P3(1)$ ,  $Z = 3$ ,  $\rho_{\text{calcd}} = 1.287$ ,  $\lambda(\text{MoK}\alpha) = 0.71073 \text{ Å}$ ,  $T = 120(2) \text{ K}$ , 26669 reflections, 8429 unique (8390 observed,  $R_{\text{int}} = 0.0426$ ),  $R_1 = 0.0875$ ,  $\omega R_2 = 0.2437$ , for 775 parameters and 19 restraints.
- [4] The sharpness of the peaks in may be explained by rapid rotation around the long axis of the tube.
- [5] A. P. Ramirez, R. C. Haddon, O. Zhou, R. M. Fleming, J. Zhang, S. M. McClure, R. E. Smalley, *Science* **1994**, *265*, 84–86.
- [6] J. D. Hartgerink, J. R. Granja, R. A. Milligan, M. R. Ghadiri, *J. Am. Chem. Soc.* **1996**, *118*, 43–50; V. Gorteau, G. Bollot, J. Mareda, D. Pasini, D.-H. Tran, A. N. Lazar, A. W. Coleman, N. Sakai, S. Matile, *Bioorg. Med. Chem.* **2005**, *13*, 5171–5180.
- [7] J. G. Morales, J. Ruez, T. Yamazaki, R. Kishan Motkuri, A. Kovalenko, H. Fenniri, *J. Am. Chem. Soc.* **2005**, *127*, 8307–8309.
- [8] V. Semetey, C. Didierjean, J.-P. Briand, A. Aubry, G. Guichard, *Angew. Chem.* **2002**, *114*, 1975–1978; *Angew. Chem. Int. Ed.* **2002**, *41*, 1895–1898; L. S. Shimizu, A. D. Hughes, M. D. Smith, M. J. Davis, B. P. Zhang, H.-C. zur Loye, K. D. Shimizu, *J. Am. Chem. Soc.* **2003**, *125*, 14972–14973.
- [9] G. Gattuso, S. Menzer, S. A. Nepogodiev, J. F. Stoddart, D. J. Williams, *Angew. Chem.* **1997**, *109*, 1615–1617; *Angew. Chem. Int. Ed. Engl.* **1997**, *36*, 1451–1454.
- [10] A. Hoffmann, D. Sebastiani, E. Sugiono, S. Yun, K. S. Kim, H. W. Spiess, I. Schnell, *Chem. Phys. Lett.* **2004**, *388*, 164–169.
- [11] V. G. Organo, A. V. Leontiev, V. Sgarlata, H. R. Rasika Dias, D. M. Rudkevich, *Angew. Chem.* **2005**, *117*, 3103–3107; *Angew. Chem. Int. Ed.* **2005**, *44*, 3043–3047; S. J. Dalgarno, G. W. V. Cave, J. L. Atwood, *Angew. Chem.* **2006**, *118*, 584–588; *Angew. Chem. Int. Ed.* **2006**, *45*, 570–574; A. N. Lazar, N. Dupont, A. Navaza, A. W. Coleman, *Chem. Commun.* **2006**, 1076–1078; A. Casnati, R. Liantonio, P. Metrangolo, G. Resnati, R. Ungaro, F. Ugozzoli, *Angew. Chem.* **2006**, *118*, 1949–1952; *Angew. Chem. Int. Ed.* **2006**, *45*, 1915–1918; M. W. Heaven, G. W. V. Cave, R. M. McKinlay, J. Antesberger, S. J. Dalgarno, P. K. Thallapally, J. L. Atwood, *Angew. Chem.* **2006**, *118*, 6367–6370; *Angew. Chem. Int. Ed.* **2006**, *45*, 6221–6224.
- [12] J. P. Hill, W. Jin, A. Kosaka, T. Fukushima, H. Ichihara, T. Shimomura, K. Ito, T. Hashizume, N. Ishii, T. Aida, *Science* **2004**, *304*, 1481–1483; S. Bhosale, A. L. Sisson, P. Talukdar, A. Fürstenberg, N. Banerji, E. Vauthey, G. Ballot, J. Mareda, C. Röger, F. Würthner, N. Sakai, S. Matile, *Science* **2006**, *313*, 84–86.